

# Theory of Alkali Induced Reconstruction of the Cu(100) Surface

S. Quassowski and K. Hermann

Fritz-Haber-Institut der Max-Planck-Gesellschaft, Faradayweg 4-6,  
D-14195 Berlin, Germany

## Abstract

LEED experiments show that Li adsorbed at Cu(100) surfaces at room temperature induces a  $(2\times 1)$  missing row substrate reconstruction while adsorption at lower temperatures,  $T=180$  K, results in an unreconstructed Cu(100)+c $(2\times 2)$ -Li overlayer structure. Substrate reconstruction has not been observed for Na nor for K adsorption. In order to study the specific reconstruction behavior of the Li adsorbate ab initio DFT calculations have been performed on Cu(100)+Ad, Ad = Li, Na, K systems at coverages  $\Theta_{\text{Ad}} = 0.25 - 0.5$  with and without reconstruction. The calculations show that the  $(2\times 1)$  MR reconstructed surface lies energetically above the ideal  $(1\times 1)$  surface by 0.2 eV per unit cell. However, alkali binding is stronger in the MR geometry as compared to that of the ideal surface where the increase in bond strength becomes smaller in going from Li to Na to K. As a result, the MR reconstructed and the overlayer adsorbate systems are energetically very close for Cu(100)+Li while for Na and K the overlayer geometry is always favored.

## 1. Introduction

It is well known from experiment that alkali adsorption at fcc(110) surfaces induces a  $(2\times 1)$  missing row (MR) substrate reconstruction (for reviews see [1, 2]). Recently, this type of adsorbate induced reconstruction was also found on fcc and bcc (100) surfaces. Examples are Au(100)+K [3], Au(100)+Na [4], Ag(100)+K [5], and Cu(100)+Li [6, 7]. Here the Cu(100)+Li system is of particular interest since it exhibits different reconstruction behavior depending on the adsorption temperature [6, 7]. At low temperatures,  $T \leq 180$  K, a c $(2\times 2)$  overlayer (OL) structure is observed for  $\Theta_{\text{Li}} \approx 0.5$  without indications of a substrate reconstruction. However, subsequent heating of the adsorbate system to room temperature leads to a  $(2\times 1)$ MR reconstruction of the Cu(100) substrate which is conserved even if the system is cooled back to 180 K. This type of adsorbate induced substrate reconstruction seems

unique for Li adsorption on Cu(100) and has not been found for larger alkali adsorbates such as Cu(100)+Na [8], Cu(100)+K [9, 10], or Cu(100)+Cs [10]. A theoretical understanding of this behavior is still lacking. In the present theoretical study we have studied the underlying mechanisms by examining differences in the alkali adsorption on ideal (1×1) and (2×1)MR reconstructed Cu(100) in order to explain the specific behavior found for Li adsorption.

## 2. Computational Details

Geometric structures of the Cu(100) substrate and of the Cu(100)+Ad, Ad = Li, Na, K adsorbate systems are described in the repeated slab geometry. The Cu substrate, in its unreconstructed (1×1) and (2×1)MR reconstructed form (see Fig. 1), is approximated by 7 and 9 layer slabs which are separated by vacuum corresponding to 5 substrate layers. This has been found to yield a reliable surface representation [11]. The alkali adsorbate layers (Li, Na, K) are added at the top and bottom of each substrate slab where for coverages  $\Theta = 0.25$  a lateral (2×2) and for  $\Theta = 0.5$  a c(2×2) and (2×1) supercell geometry is assumed as illustrated in Fig. 2a–f. The geometries of the surface systems are further optimized by allowing all atoms in the unit cells to relax according to the force field obtained from the calculations described below.

The electronic structure of the surface systems is calculated within the density functional theory (DFT) formalism using the local density approximation (LDA) [12, 13] as well as gradient corrected functionals (GGA–II) [14] for exchange and correlation. Total energies and derived quantities are obtained with the full-potential linearized augmented plane wave (FP-LAPW) method [15] implemented in the WIEN93 program [16] where 45 k-points inside the irreducible part of the Brillouin zone are used and the energy cut-off for plane wave expansions in the interstitial region is set to 9.58 Ry. Geometry optimizations of the surface systems are based on calculations of forces acting on corresponding nuclei [17] where equilibrium was assumed for forces below 3 mRy/bohr. A comparison of the geometric and energetic results from calculations using the LDA and the GGA–II approach shows only small differences which do not affect the present conclusions. Thus, we restrict ourselves in the following to results from our LDA studies.

### 3. Results and Discussion

The  $(2\times 1)$ MR reconstructed Cu(100) surface, shown in Fig. 1, is created from the ideal unreconstructed surface by removing every second row of surface atoms. As a result the top-most atoms of the reconstructed surface experience a different electronic environment which affects the surface geometry. This becomes obvious from Table 1a which gives numerical results of the present geometry optimizations. For the unreconstructed Cu(100) surface the interlayer spacing between the first and second surface layer,  $d_{12}$  ( $= 1.76 \text{ \AA}$  in the ideal bulk geometry), is decreased,  $\Delta d_{12} = -3.2\%$ , and that between the second and third layer,  $d_{23}$ , slightly increased,  $\Delta d_{23} = 0.2\%$ , in good agreement with experimental [18] and other theoretical [19] results. In contrast, the  $(2\times 1)$ MR reconstruction of pure Cu(100) yields much larger changes in the interlayer spacings:  $d_{12}$  is decreased by almost 10% and  $d_{23}$  by 2%. In the present calculations the surface energy  $\gamma$  is defined by

$$\gamma = [E_{\text{tot}}(\text{slab}, n) - E_{\text{tot}}(\text{bulk}, n)]/2 \quad (1)$$

where the total energy (per unit cell),  $E_{\text{tot}}(\text{slab}, n)$ , includes surface relaxation and reconstruction of the slab of  $n$  layers while  $E_{\text{tot}}(\text{bulk}, n)$  is obtained for the corresponding slab of the ideal bulk. For ideal  $(1\times 1)$  Cu(100) the calculations yield  $\gamma = 0.8 \text{ eV}$  while for the  $(2\times 1)$ MR reconstructed surface one finds  $\gamma = 1.0 \text{ eV}$  per  $(1\times 1)$  unit cell. Thus, the MR reconstruction requires 0.2 eV per unit cell for Cu(100) which is about 10 times larger than the energy needed for the MR reconstruction of the Cu(110) surface [20].

Table 1a compares results from geometry optimizations on the different Cu(100)+Ad, Ad = Li, Na, K adsorbate systems. Here the left part refers to overlayer structures on unreconstructed Cu(100),  $(2\times 2)$  for adsorbate coverage  $\Theta = 0.25$  (Fig. 2b) and  $c(2\times 2)$  for  $\Theta = 0.5$  (Fig. 2c) The right part shows results for adsorption on  $(2\times 1)$ MR reconstructed Cu(100), with  $(2\times 2)$  adsorbate geometry for  $\Theta = 0.25$  (Fig. 2e) and with  $(2\times 1)$  for  $\Theta = 0.5$  (Fig. 2f). Test calculations on Cu(100)+Li with different lateral adsorbate sites showed that sites of maximum coordination close to Cu substitutional sites were always energetically preferred in accordance with Figs. 2b, c, e, f. Therefore, this lateral geometry was also assumed for the Cu(100)+Na and Cu(100)+K systems.

For Cu(100)+Li the overlayer geometry (Figs. 2b, c) yields stable Li centers at  $z_{\text{Cu-Li}} = 1.8 \text{ \AA}$  above the substrate surface with only small differences between coverages  $\Theta_{\text{Li}} = 0.25, 0.5$ . This is in good agreement with recent experimental LEED results, cp. Table 1b. Further, substrate relaxation,

quantified by  $\Delta d_{12}, \Delta d_{23}$ , seems to be little influenced by adsorption as evidenced from a comparison of the theoretical Cu(100)+Li with the Cu(100) data. The overlayer geometry results for Cu(100)+Na and Cu(100)+K are found to be rather similar to those of Cu(100)+Li. Here the adsorbates stabilize for both coverages at distances  $z_{\text{Cu-Na}} = 2.1 \text{ \AA}$  and  $z_{\text{Cu-K}} = 2.5 \text{ \AA}$  above the unreconstructed Cu(100) surface. The distance values are larger than  $z_{\text{Cu-Li}}$  given above which is consistent with the increased atom size in going from Li to Na to K.

Geometry differences between the different alkalis are much more pronounced in the results for adsorption on the  $(2 \times 1)$ MR reconstructed Cu(100) surface. For Cu(100)+Li the Li atoms arrange along the Cu troughs (see Fig. 2e, f) stabilizing only slightly above the first Cu substrate layer,  $z_{\text{Cu-Li}} = 0.4 \text{ \AA}$  for  $\Theta_{\text{Li}} = 0.25$ ,  $z_{\text{Cu-Li}} = 0.2 - 0.3 \text{ \AA}$  for  $\Theta_{\text{Li}} = 0.5$ . The two different  $z_{\text{Cu-Li}}$  values given in Table 1a for  $\Theta_{\text{Li}} = 0.5$  refer to results of adjacent Li centers in rows along the Cu troughs indicating a buckling of the adsorbate layer. This is reasonable due to the fact that the Cu-Cu nearest neighbor distance which determines the lateral distance of the adsorbate rows is smaller than typical Li metal nearest neighbor distances. The increased substrate relaxation calculated for the pure  $(2 \times 1)$ MR reconstructed Cu(100) surface, see above, exists also in the Cu(100)+Li adsorbate system with variations of 3%, see  $\Delta d_{12}, \Delta d_{23}$  of Table 1a. A comparison of the theoretical relaxation data with those of the LEED experiment on Cu(100)+Li [10], cp. Table 1b, yields good agreement. The geometries calculated for Na and K adsorption on  $(2 \times 1)$ MR reconstructed Cu(100) differ considerably from those of the Cu(100)+Li system. For the lower coverage,  $\Theta = 0.25$ , the adsorbates stabilize at distances  $z_{\text{Cu-Na}} = 0.86 \text{ \AA}$  and  $z_{\text{Cu-K}} = 1.7 \text{ \AA}$  above the substrate surface which is larger than the  $z_{\text{Cu-Li}}$  value and explained by the different atom sizes. For  $\Theta = 0.5$  the adsorbate layer buckling is much more pronounced for the larger alkalis. While in Cu(100)+Li the high difference between adjacent adsorbate centers is only  $\Delta z_{\text{Cu-Li}} = 0.11 \text{ \AA}$  the calculations yield  $\Delta z_{\text{Cu-Na}} = 0.31 \text{ \AA}$  and  $\Delta z_{\text{Cu-K}} = 2.31 \text{ \AA}$ . In fact, in Cu(100)+K the theoretical buckling is so large that the concept of a smooth adsorbate layer becomes questionable.

Fig. 3 shows color coded contour plots of the charge rearrangement in the Cu(100)+alkali systems due to adsorption on the  $(2 \times 1)$ MR reconstructed substrate. The rearrangement characterizes the electronic coupling of the adsorbates with the substrate. It is quantified by the valence electron differ-

ence between the adsorbate system and its separate components

$$\Delta\rho_{val}(\mathbf{r}) = \rho_{val}(\text{Cu}(100) + \text{Ad}, \mathbf{r}) - \rho_{val}(\text{Cu}(100), \mathbf{r}) - \rho_{val}(\text{Ad}, \mathbf{r}) \quad (2)$$

where positive  $\Delta\rho_{val}$  values indicate charge accumulation and negative values depletion as a result of the adsorbate–substrate interaction. The plots refer to Li (Fig. 3a), Na (Fig. 3b), and K (Fig. 3c) coverages  $\Theta = 0.5$  and show  $\Delta\rho_{val}(\mathbf{r})$  for a planar cut perpendicular to the surface along the substrate troughs with Cu centers marked by circles and adsorbate centers by squares. Obviously, the charge rearrangement leads, for all three systems, to a depletion of charge above the (buckled) adsorbate layer which is connected with the overall positive charging of the adsorbates at the surface. The latter has been confirmed by charge integration and is to be expected from simple electronegativity arguments. Further, the plots show an almost homogeneous charge accumulation in the region between adsorbate and substrate suggesting no directional adsorbate–substrate bond formation. Thus, the alkali+Cu interaction is determined to a major degree by electrostatic and metallic contributions. Corresponding  $\Delta\rho_{val}(\mathbf{r})$  plots for the adsorption on unreconstructed Cu(100) lead to identical conclusions. These results confirm the complexity of alkali adsorption on metal surfaces which has been discussed in the literature for a long time. For reviews see Refs. [21, 22].

The relative stability of the Cu(100)–alkali systems for adsorption on the  $(2\times 1)$ MR reconstructed vs. the unreconstructed Cu(100) substrate can be determined from total energy studies. For this purpose we define a reconstruction energy  $E_s(\Theta)$  by

$$E_s(\Theta) = \gamma_{\text{rec}} - \gamma_{\text{unrec}} + D_{\text{rec}}(\Theta) - D_{\text{unrec}}(\Theta) \quad (3)$$

where  $\gamma_{\text{rec}}, \gamma_{\text{unrec}}$  denote surface energies of the pure substrate with and without reconstruction while  $D_{\text{rec}}(\Theta), D_{\text{unrec}}(\Theta)$  are adsorbate binding energies for the two substrate geometries obtained from respective total energies. Thus,  $E_s(\Theta)$  includes the energy required to reconstruct the substrate as well as the difference of adsorbate-binding with and without reconstruction. Positive  $E_s(\Theta)$  values suggest that the unreconstructed adsorbate system is energetically preferred while negative values yield the reconstructed system to be favored. Fig. 4 shows the result of the present calculations in a level diagram of  $E_s(\Theta)$  for adsorbate coverages  $\Theta = 0, 0.25, 0.5$  ( $\Theta = 0$  denotes the pure substrate). On pure Cu(100) the reconstruction energy amounts to  $E_s = 0.2$  eV per unit cell. This energy is reduced to 0.03 eV for Li and Na and to 0.05 eV for K adsorption at coverages  $\Theta = 0.25$  which demonstrates that the adsorbates are always bound more strongly to the  $(2\times 1)$ MR reconstructed

than to the unreconstructed Cu(100) substrate. At an increased coverage  $\Theta = 0.5$  the reconstruction energy is further decreased to 0.02 eV for Li adsorption. In fact, a conservative estimate of numerical errors in the calculations, yielding  $\pm 0.02$  eV, suggests that for Cu(100)+Li the reconstructed and unreconstructed systems become equally stable ( $E_s \approx 0$  eV) for  $\Theta = 0.5$ . In contrast, the reconstruction energy leads to positive values for the two larger alkali adsorbates,  $E_s(\Theta = 0.5) = 0.14$  eV for Na and  $E_s(\Theta = 0.5) = 0.19$  eV for K. This indicates that for Cu(100)+Na and Cu(100)+K adsorption on the unreconstructed substrate is energetically preferred which confirms the experimental findings [5, 9, 10].

## 4. Conclusions

The present DFT total energy studies reveal interesting details of the adsorbate induced substrate reconstruction in the Cu(100)+alkali systems. Geometry optimizations show that in Cu(100)+Li the adsorbate can stabilize on the  $(2 \times 1)$  MR reconstructed surface above the substrate troughs where the adsorbate-substrate binding is stronger compared to adsorption on the unreconstructed surface. As a result, the adsorbate systems with and without substrate reconstruction become equally stable for coverages  $\Theta = 0.25 - 0.5$  and transitions between the two becomes possible with varying temperature confirming the experimental findings [6, 7]. In contrast, calculations on the Cu(100)+Na and Cu(100)+K systems show that, for coverages  $\Theta = 0.25 - 0.5$ , adsorption on the unreconstructed Cu(100) surface is always energetically preferred over that on a (fictitious)  $(2 \times 1)$  MR reconstructed surface, again confirming the experiment [5, 9, 10]. Based on the calculations, this different behavior between the alkali adsorbates can be explained in parts by simple geometric effects. The larger alkalis, Na, K, cannot stabilize close enough to the reconstructed substrate surface and their atom sizes lead to strong layer buckling for higher adsorbate coverages which makes adsorption on the reconstructed substrate very unlikely to occur. It should be emphasized that the present calculations refer to static equilibrium structures of Cu(100)+alkali which can be compared for different constraints, overlayer or missing row. Transition states between the different structures and respective energy barriers require the knowledge of appropriate reaction paths which have to be assumed or obtained from separate ab initio molecular dynamics calculations.

## **Acknowledgment**

This study was supported in parts by Deutsche Forschungsgemeinschaft (Sonderforschungsbereich 290, Berlin).

## References

- [1] H. Over, H. Bludau, M. Gierer, and G. Ertl, *Surf. Rev. Lett.* **2**, 409 (1995).
- [2] R. D. Diehl and R. McGrath, *Surf. Rev. Lett.* **2**, 387 (1995).
- [3] M. Okada, H. Iwai, R. Klauser, and Y. Murata, *J. Phys. C* **4**, L593 (1992).
- [4] A. Neumann, S. L. M. Schroeder, and K. Christmann, *Phys. Rev. B* **51**, 17007 (1995).
- [5] M. Okada, H. Tochihara, and Y. Murata, *Surf. Sci.* **245**, 380 (1991).
- [6] H. Tochihara and S. Mizuno, *Surf. Sci.* **279**, 89 (1992).
- [7] S. Mizuno, H. Tochihara, and T. Kawamura, *Surf. Sci.* **292**, L811 (1993).
- [8] A. Reichmuth, Master's thesis, University Göttingen, 1991.
- [9] T. Augura, H. Tochihara, and Y. Murata, *Surf. Sci.* **158**, 490 (1985).
- [10] H. L. Meyerheim, J. Wever, V. Jahns, W. Moritz, P. J. Eng, and I. K. Robinson, *Surf. Sci.* **304**, 267 (1994).
- [11] S. Quassowski and K. Hermann, to be published (unpublished).
- [12] D. Ceperley and B. Alder, *Phys. Rev. B* **45**, 566 (1980).
- [13] J. Perdew and A. Zunger, *Phys. Rev. B* **23**, 5048 (1981).
- [14] J. P. Perdew, J. A. Chevary, S. H. Vosko, K. A. Jackson, M. R. Pederson, D. J. Singh, and C. Fiolhais, *Phys. Rev. B* **46**, 6671 (1992).
- [15] O. K. Andersen, *Phys. Rev. B* **12**, 3060 (1975).
- [16] P. Blaha, K. Schwarz, P. Soratin, and S. B. Trickey, *Comput. Phys. Commun.* **59**, 399 (1990).
- [17] B. Kohler, S. Wilke, M. Scheffler, R. Kouba, and C. Ambrosch-Draxl, *Comput. Phys. Commun.* **94**, 31 (1996).
- [18] D. E. Fowler and J. V. Barth, *Phys. Rev. B* **52**, 2117 (1995).
- [19] T. Rodach, K.-P. Bohnen, and K. Ho, *Surf. Sci.* **286**, 66 (1993).



- [20] G. Vielsack and M. Scheffler, to be published (unpublished).
- [21] *Physics and Chemistry of Alkali Metal Adsorption*, edited by H. P. Bonzel, A. M. Bradshaw, and G. Ertl (Elsevier, Amsterdam, 1989).
- [22] C. Stampfl and M. Scheffler, *Surf. Rev. Lett.* **2**, 317 (1995).
- [23] S. Mizuno, H. Tochiyama, and T. Kawamura, *Surf. Sci.* **293**, 239 (1993).

## Tables

Table 1.

Geometry results of the Cu(100) substrate and of the Cu(100)+Ad, Ad = Li, Na, K adsorbate systems with and without substrate reconstruction and for adsorbate coverages  $\Theta = 0.25 - 0.5$ . Table 1a lists theoretical data from the present LDA calculations and from those of ref. [19] while Table 1b compares experimental data of refs. [7], [10], [19], [18], [23]. For definitions of the (differential) perpendicular distances,  $z_{\text{Cu-Ad}}$ ,  $\Delta d_{12}$ ,  $\Delta d_{23}$ , see text.

	Overlayer structure			Missing row reconstruction		
Coverage $\Theta$ (ML)	$z_{\text{Cu-Ad}}$ ( $\text{\AA}$ )	$\Delta d_{12}$ (%)	$\Delta d_{23}$ (%)	$z_{\text{Cu-Ad}}$ ( $\text{\AA}$ )	$\Delta d_{12}$ (%)	$\Delta d_{23}$ (%)
<b>(a) Theory:</b>						
<b>Cu(100)</b>						
0.0	–	–3.2	+0.2	–	–9.6	–2.1
0.0 [19]	–	–3.0	+0.1	–	–	–
<b>Cu(100)+Li</b>						
0.25	1.82	–4.0	–2.7	0.42	–12.2	–3.4
0.50	1.81	–2.7	–1.9	0.20/0.31	–8.2	–1.8
<b>Cu(100)+Na</b>						
0.25	2.09	–4.8	–4.3	0.86	–13.1	–3.8
0.50	2.12	–4.1	–4.0	0.62/0.93	–9.2	–3.5
<b>Cu(100)+K</b>						
0.25	2.48	–4.8	–3.2	1.27	–9.3	–3.5
0.50	2.56	–4.3	–4.7	1.16/3.47	–9.9	–3.4
<b>(b) Experiment:</b>						
<b>Cu(100)</b>						
0.0 [18]	–	$-2.0 \pm 0.2$	$+0.5 \pm 1.2$	–	–	–
<b>Cu(100)+Li</b>						
0.25 – 0.55 [7, 23]	$1.96 \pm 0.08$	$0 \pm 2$	–	–	$-7 \pm 3$	$0 \pm 2$
<b>Cu(100)+K</b>						
0.25 [10]	$2.25 \pm 0.15$	–	–	–	–	–

## Figure Captions

Fig. 1

Perspective view of the Cu(100) surface showing the ideal (1×1) and the (2×1) missing row reconstructed geometry. The two-dimensional elementary cells are marked by rectangles for each geometry.

Fig. 2

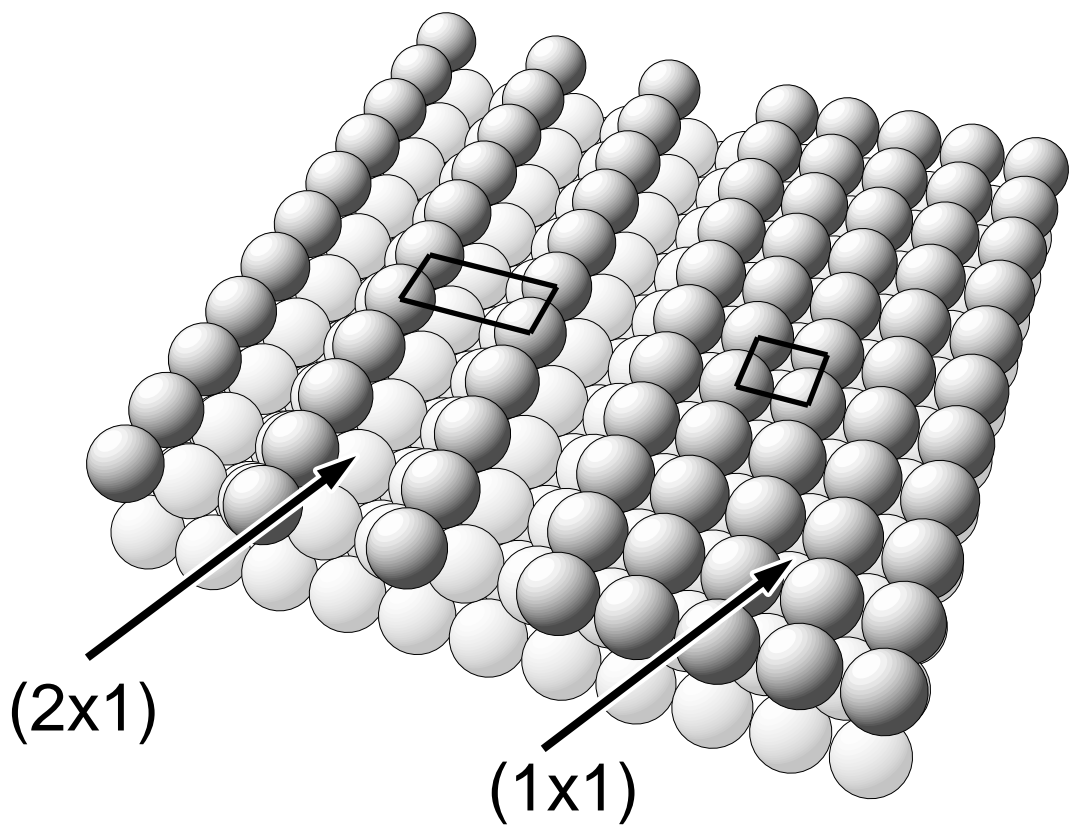
Top view of the pure Cu(100) and of the adsorbate covered Cu(100)+alkali surfaces illustrating different surface geometries considered in the present study. The Cu substrate atoms are shown as dark (1st layer) and light (2nd, 3rd layer) gray balls while the alkali adsorbate atoms are indicated by red balls. The upper part of Fig. 2 refers to adsorption on the unreconstructed Cu(100) surface showing (a) the ideal (1×1) substrate, (b) (2×2) adsorption ( $\Theta = 0.25$ ), and (c) c(2×2) adsorption ( $\Theta = 0.5$ ). The lower part refers to adsorption on the reconstructed surface showing (d) the (2×1) missing row substrate, (e) (2×2) adsorption ( $\Theta = 0.25$ ), and (c) (2×1) adsorption ( $\Theta = 0.5$ ).

Fig. 3

Color coded contour plots of the charge density difference,  $\Delta\rho_{val}(\mathbf{r})$ , of Cu(100) covered with alkali adsorbates (a) Li, (b) Na, and (c) K. The plots refer to the (2×1) missing row reconstructed substrate and adsorbate coverages  $\Theta = 0.5$  and show  $\Delta\rho_{val}(\mathbf{r})$  for a planar cut perpendicular to the surface along the substrate troughs. For a definition of  $\Delta\rho_{val}(\mathbf{r})$  see text. The units used for the color coding, see right scale, are  $1/\text{bohr}^3$ .

Fig. 4

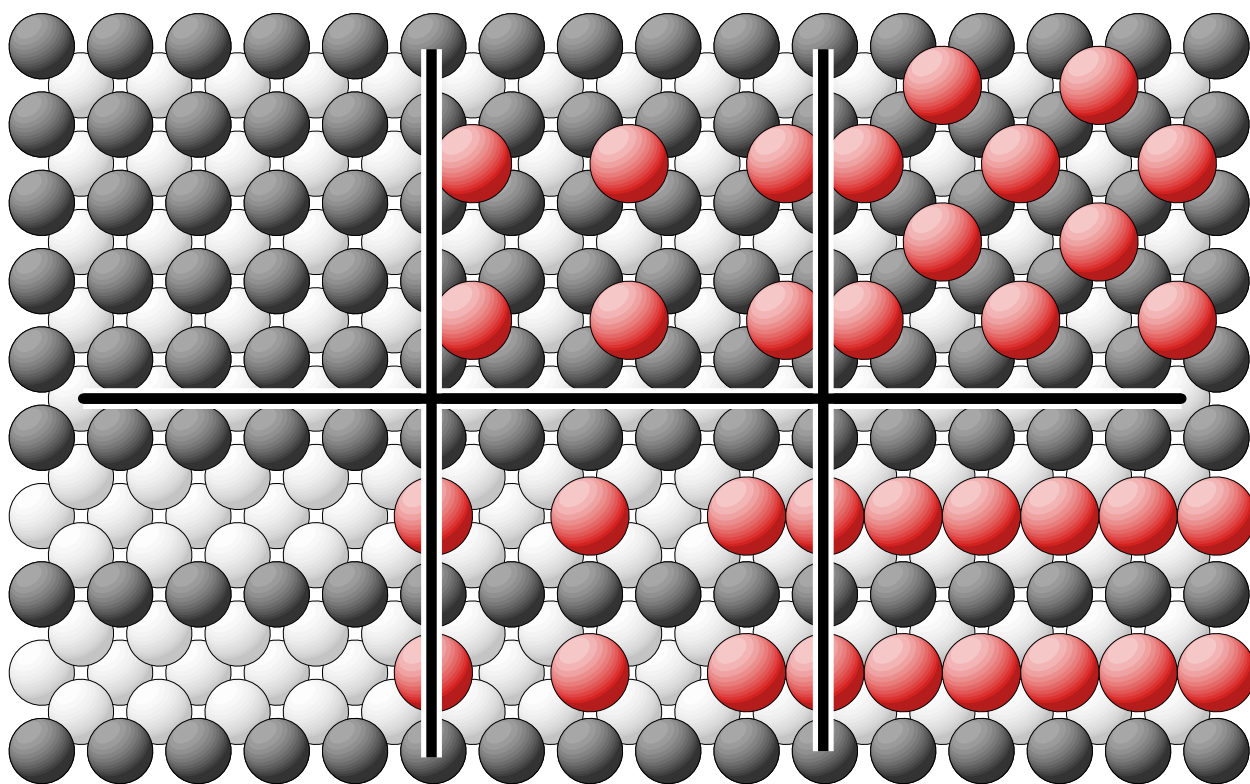
Level diagram of the reconstruction energy  $E_s(\Theta)$  for the Cu(100)+Ad, Ad = Li, Na, K systems at adsorbate coverages  $\Theta = 0, 0.25, 0.5$  ( $\Theta = 0$  denotes the pure substrate). For a definition of  $E_s$  see text. The error bar of  $\pm 0.02$  eV shown with the Li result for  $\Theta = 0.5$  gives an estimate of numerical errors in the calculations.



(a)

(b)

(c)

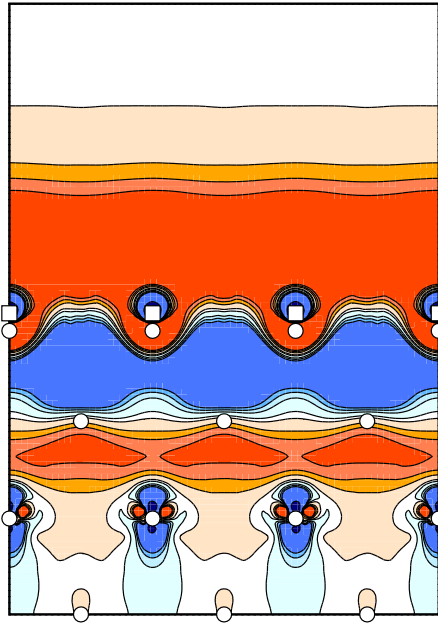


(d)

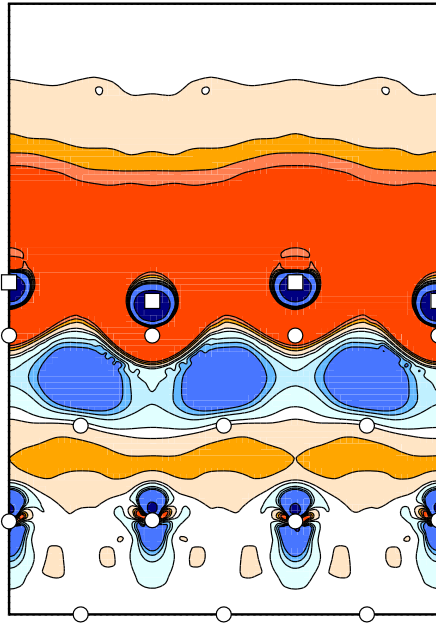
(e)

(f)

(a)



(b)



(c)

